Structural characterization of Si_mGe_n strained layer superlattices

P. M. Adams and R. C. Bowman, Jr.[a)]
The Aerospace Corporation, P. O. Box 92957, Los Angeles, California 90009

C. C. Ahn
W. M. Keck Laboratory, California Institute of Technology, Pasadena, California 91125

S. J. Chang, V. Arbet-Engels, M. A. Kallel, and K. L. Wang
Device Research Laboratory, Electrical Engineering Department, University of California, Los Angeles, California 90024

(Received 18 October 1991; accepted for publication 29 January 1992)

Si_mGe_n strained layer superlattice (SLS) structures were grown by molecular beam epitaxy on Ge_xSi_{1-x} buffer layers on ⟨100⟩ Si substrates to determine the effects of buffer layer composition, SLS thickness ratio, and superlattice periodicity, on the overall quality of these structures. X-ray diffraction methods were used to determine how closely actual periodicities and compositions met targeted values, and to evaluate the quality of these samples. In most instances the as-grown structures matched the targeted values to within 10%, though in some instances deviations of 20–25% in either the period or composition were observed. The quality of the SLS structures was greatly dependent on the composition of the buffer layer on which it was grown. Si_mGe_n SLS structures grown on Si- and Ge-rich buffer layers were of much higher quality than Si_mGe_m SLSs grown on $Ge_{0.50}Si_{0.50}$ layers, but the x-ray rocking curves of the Si_mGe_n samples indicated that they were far from perfect and contained moderate levels of defects. These results were confirmed by cross sectional transmission electron microscopy, which showed that the Si_mGe_m structures contained significant numbers of dislocations and that the layers were nonuniform in thickness and wavy in appearance. Si_mGe_n structures, however, displayed fewer defects but some dislocations and nonparallelism of layers were still observed.

I. INTRODUCTION

With advances in silicon molecular beam epitaxy (Si-MBE) the growth of high quality Si/Ge layers has become possible. The large lattice mismatch (4.2%) between Si and Ge permits heteroepitaxial layers to be grown under a variety of controlled strain conditions and a number of devices based on Ge_xSi_{1-x} layers have been proposed and grown.[1] Through band gap engineering, the fabrication of novel electro-optic devices, based on Si_mGe_n strained layer superlattices (SLS) has been suggested, and much effort has been directed to the growth of these structures.[2–4] These structures are composed of alternating pure Si (m monolayers) and pure Ge (n monolayers) grown on a Ge_xSi_{1-x} buffer layer, but the large mismatch between Si and Ge places severe constraints on the design of these devices because of the very small critical thickness for pseudomorphic growth.

While a number of novel device structures have been fabricated, not all attempts at measuring the predicted optical and electrical properties have been successful. It has not been demonstrated whether the quality of the material was adequate to produce the predicted properties, or if the quality may be a function of the compositions and actual structures grown. For this reason, a series of Si_mGe_n SLS structures were grown by MBE on ⟨100⟩ Si substrates as part of a study to determine the effects of buffer layer composition, SLS thickness ratio (i.e.; m:n), and superlattice periodicity, on the overall quality of these structures, and their optical properties. Table I summarizes the target configurations of the SLS structures evaluated. Buffer layer compositions of $x = 0.20$, 0.50, and 0.80 were selected and layer thicknesses were chosen to be well above the critical thickness for each composition. The Si:Ge thickness ratios in the SLSs ranged from 4:1 to 1:1 to 1:4 in order to establish strain symmetrization[2] with respect to each buffer layer composition. The superlattice periodicity varied from 10 ($m+n$) monolayers (~1.4 nm) to 40 monolayers (~5.6 nm) and the number of SLS periods were adjusted to give a total SLS thickness of approximately 300 nm in each case.

II. STRUCTURE AND CHARACTERIZATION OF Ge_xSi_{1-x} LAYERS AND Si_mGe_n SLSs

Up to the critical thickness, Ge_xSi_{1-x} layers grown on Si substrates undergo a tetragonal distortion, whereby the lattice parameter of the layer parallel with the surface matches that of the substrate, while the lattice parameter perpendicular to the surface is elastically strained. The strained perpendicular lattice parameter of a Ge_xSi_{1-x} layer can be related to the relaxed lattice parameter by[5]

$$a_r = K(a_s - a_0) + a_0, \tag{1}$$

where a_r and a_s are the relaxed and strained lattice parameters of the layer respectively, a_0 is the lattice parameter of the Si substrate (0.54309 nm), and K is a constant (0.565

[a)]Present address: Aerojet Electronic Systems Division, P. O. Box 296, Azusa, CA 91702.

 0021-8979/92/094305-09$04.00

TABLE I. Comparisons of target parameters for Si_mGe_n superlattices grown on ⟨100⟩ Ge_xSi_{1-x} buffer layers with experimentally determined values.

SLS structure	Buffer layer composition (x)			Buffer layer thickness (nm)		SLS target		SL periodicities (nm)				
		Measured[a]										
	Target	Buffer	SL	Target	Measured[b]	Thickness	Periods	Target	LA XRD[c]	HA XRD[c]	Raman	TEM
$Si_{32}Ge_8$	0.20	0.15	0.15	2000	1680	336	60	5.6	5.0	5.4	5.6	4.9
Si_8Ge_{32}	0.80	0.78	0.78	800	690	336	60	5.6	5.6	6.1	6.0	5.8
$Si_{20}Ge_{20}$	0.50	0.49	0.39	200	160	308	55	5.6	4.2	5.0	5.5	4.8
$Si_{15}Ge_{15}$	0.50	0.52	0.42	200	147	307	73	4.2	3.1	3.5	3.8	3.2
$Si_{10}Ge_{10}$	0.50	0.43	0.53	200	151	308	110	2.8	2.1	2.3	2.4	1.9
Si_5Ge_5	0.50	0.47	0.42	200	184	304	217	1.4	1.4	1.4	1.5	1.4
$Si_{16}Ge_4$	0.20	0.14	0.14	2000	1890	336	120	2.8	2.8	3.0	···	2.7
Si_4Ge_{16}	0.80	0.80	0.74	800	730	336	120	2.8	2.5	2.7	···	2.4

[a]From $k_{\alpha 2}$ stripped θ-2θ scans.
[b]From XTEM images.
[c]From low and high angle θ-2θ scans.

for ⟨100⟩ substrates). From Vegard's law the composition (x) of the layer can be related to the relaxed lattice parameter by

$$x = 1 - [(a_g - a_r)/(a_g - a_0)], \tag{2}$$

where a_g is the relaxed lattice parameter of Ge (0.56576 nm). Above the critical thickness, defects such as threading and misfit dislocations are introduced and the Ge_xSi_{1-x} layers subsequently relax. One way of increasing the critical thickness of pure Ge layers grown on Si substrates is to introduce a buffer layer of intermediate composition (Ge_xSi_{1-x}) between the substrate and a Ge layer or Si_mGe_n SLS structure. By selecting the thickness of the buffer layer to be sufficiently above the critical thickness, the layer can be assumed to be completely relaxed. If the average composition of a Si_mGe_n SLS structure is chosen to match that of the buffer, then the strain in the structure will be shared between both the Si and Ge layers and represents a state of strain symmetrization.[2] As a result, the parallel lattice parameters of the Si and Ge layers in the SLS are identical and match that of the buffer layer. The Si and Ge layers, however, both undergo a tetragonal distortion and the perpendicular lattice parameters can be predicted from elasticity theory (e.g., Ref. 5.) assuming that the parallel lattice parameters for the layers match that of the buffer, which now acts as a substrate.

In order for the novel properties of Si_mGe_n structures to be realized, it is important that the SLS be relatively defect free and that interfaces be sharp. X-ray diffraction (XRD) is a technique that has been used to evaluate the lattice mismatch, composition, and state of relaxation in Ge_xSi_{1-x} layers and characterize the quality of multilayer Si-Ge_xSi_{1-x} and Si_mGe_n superlattice structures.[6–9]

Reference 10 gives an overview of the diffraction effects that are produced by the interaction of x rays with artificially modulated structures. In summary, the layers in the superlattice act as artificial planes for Bragg diffraction and produce a series of peaks in the low angle 2θ region whose positions can be approximated from Bragg's law

$$n\lambda = 2P \sin\theta, \tag{3}$$

where λ is the x-ray wavelength, P is the superlattice period, θ is the angle between the lattice planes and the incident x-ray beam, and n is an integer. The period of the superlattice can be determined from Eq. (3) and the overall quality of the superlattice, including the sharpness of interfaces, uniformity in layer thicknesses, and dislocation density will be a function of the number of higher order ($n = 1,2,3,...$) reflections that are observed. Since the Si_mGe_n multilayers are heteroepitaxial, a series of superlattice satellite reflections are associated with the reflections from the Si substrate. For the (400) reflection, the zero-order superlattice reflection, whose position is related to a unit cell with the mean lattice parameter in the structure, is determined by the average strains and is given by[11]

$$-\Delta\theta_0 = k_1 e_\perp + k_2 e_\parallel, \tag{4}$$

where

$$k_1 = \cos^2\psi \tan\theta_B \pm \sin\psi\cos\psi,$$

$$k_2 = \sin^2\psi \tan\theta_B \pm \sin\psi\cos\psi,$$

and $\Delta\theta_0$ is the separation between SL and substrate reflections, ψ is the angle between lattice planes and sample surface, θ_B is the Bragg angle of the substrate, and $e_\perp$ and $e_\parallel$ are respectively, the average perpendicular and parallel strain in the structure with respect to the Si substrate. The period of the superlattice can also be determined from the spacing of the high angle satellite peaks and is given by[11]

$$P = \lambda\gamma_h/\Delta\theta_p \sin 2\theta_B, \tag{5}$$

where γ_h is the direction cosine between the diffracted beam and sample surface inward normal, and $\Delta\theta_p$ is the separation between superlattice reflections.

The large lattice mismatch between Si and Ge and the range of periods of interest in Si_mGe_n SLSs permits routine XRD analysis with a conventional powder diffractometer (θ-2θ scans). However, as the name implies this instrument was not designed for analyzing single crystals and care must be taken in conducting XRD analyses so as to minimize the introduction of artifacts and an awareness must be developed for the limitations of the technique. In

θ-2θ scans a diffracted signal is only recorded from those lattice planes aligned parallel with the sample surface, which is assumed to be aligned along the diffractometer axis and symmetric with respect to the incident and diffracted x-ray beams. Single crystal samples, however, can potentially be cut off-axis by varying amounts and the degree of misorientation can effect the intensity of the diffracted signal. This effect is further complicated by the fact that the divergence of the x-ray beam is different in the axial and equatorial directions.[12] As a result, sample misorientation will influence the XRD profile and the effect will be dependent on the sample's azimuthal orientation in the instrument.

Double-crystal x-ray rocking curves provide much higher resolution than θ-2θ scans and are more sensitive to a wider range of defects present in single crystals. In addition, other adjustments are typically available on this instrument which enable a more accurate alignment of the sample, thereby eliminating the problem encountered with off-axis samples. The main limitations of the double-crystal instrument, with respect to the powder diffractometer, are its limited scanning range ($\sim 5.5°$ $\Delta\theta$) and much lower intensity x-ray beam. A combination of analyses utilizing both XRD techniques, therefore, has advantages for characterizing the structure and overall quality of Si_mGe_n superlattices.

Cross sectional transmission electron microscopy (XTEM) can image interfaces and structures at very high resolution and allow characterization of the quality of SLSs through the identification of defects. It thereby complements XRD measurements, which are sensitive to the levels of defects but cannot identify their exact nature.

Raman spectroscopy provides an additional nondestructive method for evaluating the quality of Si-Ge layers and SLS structures. For example, the interface abruptness can be estimated from the relative intensity of the Ge-Si phonon vibration as well as the energy positions of the Ge-Ge and Si-Si phonon peaks. Furthermore, the superlattice period can be calculated by applying Rytov's elastic continuum model for vibrations in layered media.[13]

Rutherford backscattering spectroscopy (RBS) can also be used to obtain the average composition of buffer layers and SLSs and has advantages over XRD methods since its measurements are independent of, and do not require any assumptions regarding the state of strain in the epitaxial layers.

III. EXPERIMENT

The samples studied in this work were grown in a Perkin–Elmer MBE system equipped with separate electron beam evaporators for Si and Ge, a quadrupole mass spectrometer for residual gas analysis, and a reflection high-energy electron diffraction (RHEED) system for *in situ* monitoring of the film quality. The details of the growth of the Si_mGe_n samples are summarized from Refs. 14 and 15. The base and growth pressures were $7–8\times10^{-11}$ and $5–9\times10^{-9}$ Torr, respectively, and the fluxes of the Si and Ge sources were monitored with an Inficon Sentinel III controller. The growth temperatures/growth rates ranged from 380 °C/0.05 nm s^{-1} to 550 °C/0.1 nm s^{-1} for the SLSs and buffer layers, respectively.

Theta two-theta XRD scans were performed using copper radiation on a computer controlled powder diffractometer equipped with a theta compensating slit and diffracted beam monochromator. X-ray rocking curves were obtained with a commercially available double-crystal diffractometer using copper $k_{\alpha 1}$ radiation. A $\langle 100 \rangle$ germanium crystal set for the (400) reflection served as a monochromator and a set of slits were used to limit the incident x-ray beam size to approximately 0.50 mm^2 and exclude the $k_{\alpha 2}$ component from the monochromator.

Sample preparation for XTEM analysis followed standard procedures, including the mechanical thinning and polishing of thin sections, followed by dimpling to perforation and Ar ion milling. Specimens were examined in a Philips Electronics Instruments model 430 STEM operated at 300 kV under bright field and dark field conditions.

Raman scattering spectroscopy was performed at room temperature with a near-backscattering geometry and the details are summarized from Refs. 14 and 15. Samples were kept in vacuum in order to reduce stray light scattering from the air. Various lines (457.9, 488.0, 514.5 nm) from an argon ion laser were used for excitation and the scattered light was analyzed with a Spex 1404 double-monochromator and an EG&G Ortec 941 photon counter.

Rutherford backscattering measurements were made with 3 MeV $^4He^{++}$ using the California Institute of Technology Tandem accelerator.

IV. RESULTS

A. X-ray diffraction

The measurements of buffer layer compositions and SL periodicities made from the XRD analyses are summarized in Table I and preliminary data on the quality of the SLSs have been presented in Ref. 16. The low angle θ-2θ XRD scans for the nominal 40 monolayer (ML) and 20 ML period SLSs are presented in Figs. 1 and 2, respectively. It can be seen that the quality of the SLSs, as expressed by the number of higher-order harmonics, varies depending on the composition of the buffer layer. From both the low angle and high angle (400) θ-2θ scans it is evident that the quality of the Si_mGe_m SLSs grown on the $Ge_{0.50}Si_{0.50}$ buffer layers are of much poorer quality than those on both the low ($x = 0.20$) and high ($x = 0.80$) germanium content buffer layers. For both the 20 and 40 ML period Si_mGe_m SLSs only two orders of superlattice reflections were observed in the low angle scans. This is in contrast with up to six and nine orders of reflections being observed for the 40 ML period Si_mGe_n SLSs and four and five orders for the corresponding 20 ML period SLSs. Additional differences in quality were observed between some of the Si_mGe_n SLSs as indicated by the number of higher-order reflections and the full width half maximum (FWHMs) of the superlattice peaks. The most noticeable difference existed between the $Si_{32}Ge_8$ and Si_8Ge_{32} SLSs, with the Ge-rich sample exhibiting much narrower (0.07° 2θ) and more higher-order superlattice reflections. A similar trend, however, was not

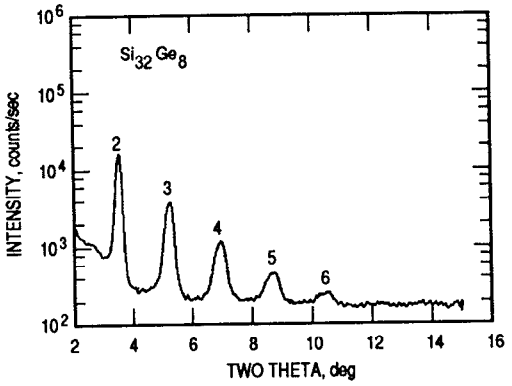

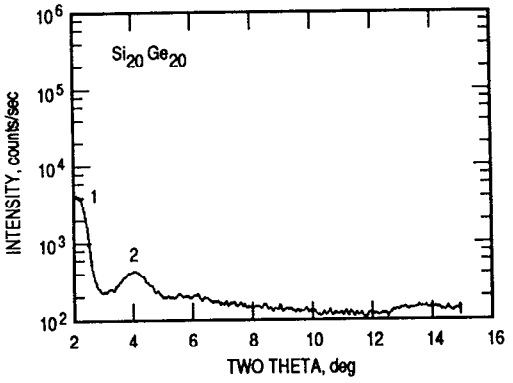

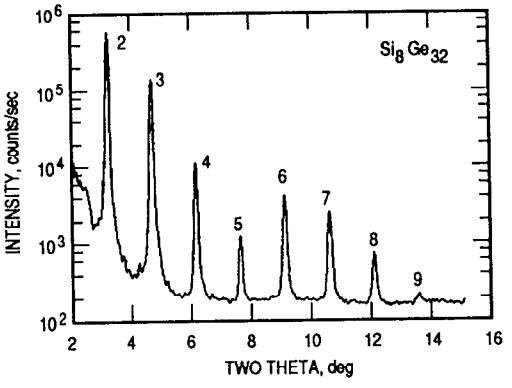

FIG. 1. Low angle θ-2θ x-ray diffraction scans from nominal 40 monolayer period SLSs.

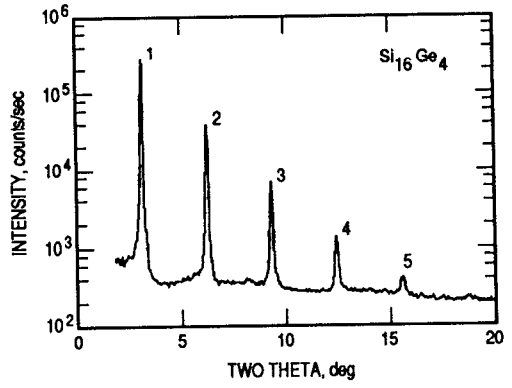

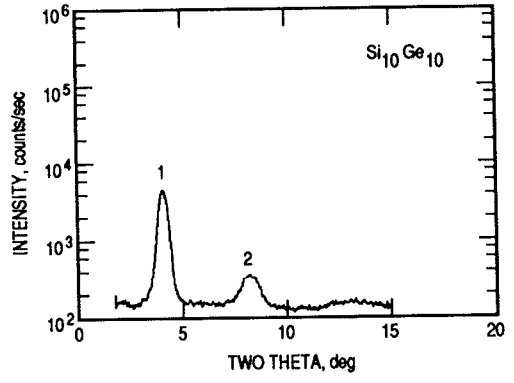

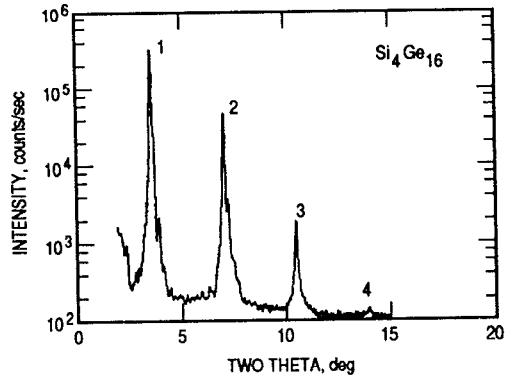

FIG. 2. Low angle θ-2θ x-ray diffraction scans from nominal 20 monolayer period SLSs.

observed with the 20 ML period structures. Therefore, this effect does not appear to be solely dependent on the buffer layer composition, and other factors such as incomplete relaxation of the buffer layer during growth, the degree of lattice mismatch between the buffer and SLS, or differences in growth conditions may also have had an influence.

The (400) x-ray rocking curves of the 40 ML SLSs are given in Fig. 3 and present a much clearer indication of the quality of the structures. The rocking curves of the 20 ML samples are comparible in appearance. For both the 20 ML and 40 ML SLSs the -1 order reflection of the Si_mGe_m samples was either absent or extremely broad, whereas weak broad -1 order SLS reflections were observed for the corresponding Si_mGe_n structures. This is consistent with the θ-2θ results, which indicated that the SLSs grown on the $Si_{0.50}Ge_{0.50}$ buffer layers were of poorer quality.

It was noted that the FWHMs of both the Si-rich buffer peaks are nearly half (0.16 vs 0.32° $\Delta\theta$) those of the Ge-rich buffers and the FWHMs of the -1 superlattice reflections are slightly larger than, but otherwise closely match, those of the buffer layers. In addition, the intensities of the -1 order SL reflections from both of the Si-rich SLS samples are comparable, and considerably less than those of the corresponding Ge-rich specimens. This is probably a result of the Ge-rich SLSs having a larger structure factor as a consequence of the greater scattering power of Ge.

The FWHM of the rocking curve has been related to the dislocation density by[17]

$$D = (\mathrm{FWHM}^2/9b^2)\times(1\times10^{14}), \tag{6}$$

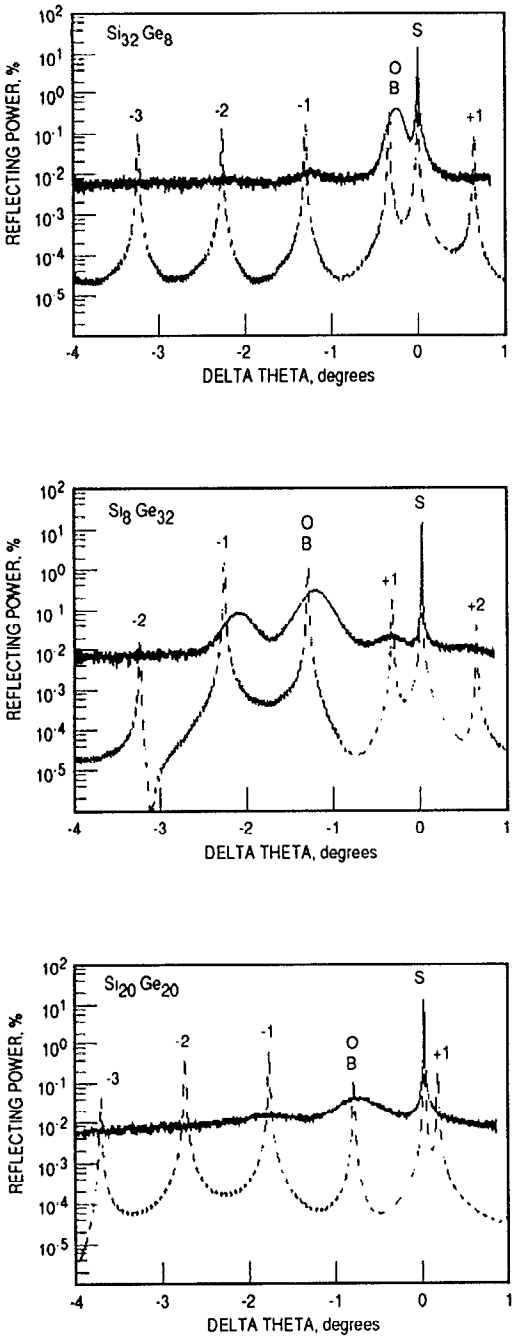

FIG. 3. Experimental (solid) and calculated (dashed) (400) rocking curves from nominal 40 monolayer period SLS structures.

where D is the dislocation density (cm^{-2}), FWHM is the full width at half maximum of the rocking curve (in rads), and b is the Burger's vector ($a_0/2\langle 110\rangle = 0.4$ nm for 60° type dislocations). The observed FWHMs imply that dislocation densities are lower in the Si-rich buffers than in the Ge-rich buffer layers. Dislocation densities calculated from this relationship range from 5×10^8 cm^{-2} to 2×10^9 cm^{-2} for the Si- and Ge-rich buffer layers, respectively. This is consistent with the relaxation mechanism of the buffer layers, whereby fewer threading dislocations would be required to relax a Si-rich buffer than a Ge-rich buffer on a Si substrate. The fact that the FWHMs of the observed SL reflections are similar to those of the buffer layers suggests that defect levels are comparable.

The results from the θ-2θ XRD scans have indicated that the qualityof the Si_mGe_n structures is considerably greater than that of the Si_mGe_m SLSs; however, the x-ray rocking curves suggest that significant numbers of defects are nevertheless present in these structures. One potential method for evaluating the quality and state of strain in a SLS is by simulating the rocking curve from a trial structure using a kinematical model for x-ray diffraction[18] and comparing the results with the those observed from the sample. An iterative procedure of adjusting the trial structure until the calculated rocking curve matches the observed pattern may yield a reasonable approximation to the actual state of strain in the SLSs structure. In modeling the rocking curves the SLS structures were assumed to have the nominal targeted periodicities, to be completely symmetrically strained, and to have a high degree of perfection. The relaxed buffer layers were not modeled in the simulations. The presence of defects and their effects in the x-ray rocking curves are clearly shown in Fig. 3 which compares the curves obtained from the 40 ML samples with those calculated, as described above, for defect-free strain symmetrized structures. The broad nature of the SL reflections and the limited number of harmonics that were recorded in the rocking curves indicate that the best Si_mGe_n SLSs that we have studied are far from defect free and not as good as would have been expected strictly from the θ-2θ scans.

In selecting the Si:Ge ratio for a perfectly strain symmetrized SLS the average composition of the SLS should match that of the buffer layer and the strain should be shared between the Si and Ge layers. As a result, if there is exact lattice matching of the SLS to the buffer layer and the SLS has the correct stoichiometry, then the (400) reflection of the buffer layer should coincide with the 0-order (400) reflection of the SLS. We have used stripping of the $k_{\alpha 2}$ component[19] from the θ-2θ scans to improve the resolution in the vicinity of the (400) reflection and the positions of peaks in these scans were used in calculating the compositions of the buffer layers and SLS's. The results have been presented in Table I. The measured compositions of the buffer layers in most cases closely agreed with the targeted values, but those with the lowest targeted Ge contents ($x = 0.20$) deviated the greatest, with compositions 25% lower than expected. Figure 4 presents the $k_{\alpha 2}$ stripped scans for the $Si_{15}Ge_{15}$ and $Si_{32}Ge_8$ structures. In the θ-2θ scans of the $Si_{15}Ge_{15}$ SLS, and to a lesser extent the $Si_{20}Ge_{20}$, $Si_{10}Ge_{10}$, Si_5Ge_5, and Si_4Ge_{16} samples, two distinct peaks or peaks with shoulders were observed at the position of the buffer layer/0-order SL (400) reflection. In comparison, the scan of the $Si_{32}Ge_8$ sample displayed a single peak indicating a good level of lattice matching between the buffer and SLS. When multiple peaks were present it was possible to calculate the average composition of both the buffer layer and SLS. The SLS peak was discriminated from the buffer by using the positions of the SLS satellite reflections to predict the most likely location

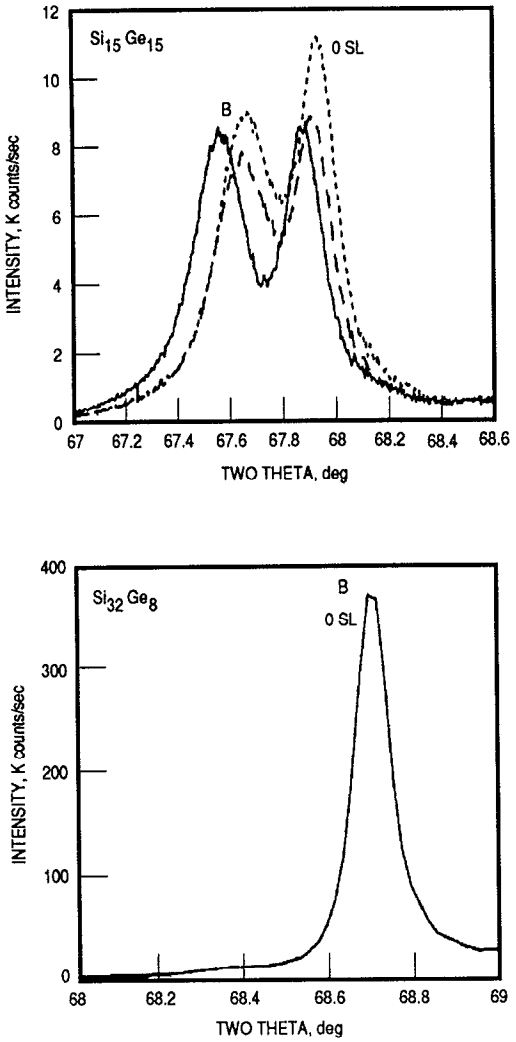

FIG. 4. $k_{\alpha 2}$ stripped θ-2θ XRD scans of (400) reflection from buffer layers(B) and 0-order SL reflection from $Si_{15}Ge_{15}$ and $Si_{32}Ge_8$ SLSs. Solid, dotted, and dashed lines refer to as grown, 880 °C/9 s, and 935 °C/20 s anneal samples, respectively.

of the 0-order SL reflection. The (400) rocking curves of these samples, however, show single peaks whose FWHMs are all substantially greater (2–3×) than in the θ-2θ scans as a result of their recording the full range of mosaic spread. While the θ-2θ scans do not give a true indication of the quality of the structures they may provide a form of artificially higher resolution than the rocking curves and allow additional insight into the structure of the SLSs and the degree of lattice matching with the buffer layers.

The presence of separate buffer and 0-order SLS (400) reflections in several samples implies that the average strains in the SLSs and buffers are substantially different. It is interesting, however, to compare the periodicities targeted for strain symmetrization and those actually observed (Table I). In most cases the measured and targeted values agree to better than 10%, but those of the $Si_{10}Ge_{10}$ and $Si_{15}Ge_{15}$ samples differ drastically; by as much as 20%. Deviations of the as-grown Si and Ge layer thicknesses from the targeted value would therefore effect

TABLE II. Comparison of Rutherford backscattering data with XRD and XTEM results.

	Composition (X_B,X_S)[a]			Thickness (T_B,T_S),[a] (nm)		
Sample		RBS	XRD		RBS	XTEM[b]
Si_8Ge_{32}	$X_B = X_S$	0.75	0.78	$T_{B+S}=$	1050	1038
$Si_{16}Ge_4$	$X_B = X_S$	0.13	0.14	$T_{B+S}=$	2250	2214
Si_4Ge_{16}	$X_B=$	0.78	0.80	$T_B=$	770	730
	$X_S=$	0.75	0.74	$T_S=$	330	288

[a]Subscripts B and S refer to buffer and superlattice, respectively.
[b]Total thickness of SLS calculated from (average period) × (number of periods).

both the average strain in the structures and the periodicities; however simple errors in the thicknesses of only the Si or Ge layers from the targeted values do not appear to account for the observed periodicities and average SLS compositions. In contrast to the samples grown on the intermediate composition buffer layers, the Si_mGe_n samples displayed much narrower (400) buffer/0-order SL reflections, and with the exception of the Si_4Ge_{16} structure only single peaks were observed. This implies that the lattice matching between the SLSs and buffer layers was much better in these samples, and similarly the observed SL periodicities were in reasonably good agreement ($<7\%$) with the targeted values (see Table I).

Rutherford backscattering analyses were performed on three of the samples as an independent measure of the average SLS and buffer layer compositions. A comparison of the RBS data with the compositions derived by XRD is given in Table II. In two of the samples (Si_8Ge_{32},$Si_{16}Ge_4$) the compositions of the buffers and SLSs were indistinguishable. In the Si_4Ge_{16} sample, however, a difference in composition was observed which was consistent with the XRD results. The RBS and XRD compositions, in several instances, agreed to within 0.01 wt % Ge, which is considered the limit of uncertainty in the RBS technique. Where there were more significant (>0.01) differences it was possible to calculate the degree of relaxation in the buffer layers from the lattice mismatch (XRD) and the RBS compositions and in both cases the % relaxation was on the order of 95–97%. This is reasonably consistent with the buffer layers being completely or nearly completely relaxed and justifies this assumption in calculating the compositions from the XRD data.

A series of rapid thermal annealing experiments were conducted with several of these samples[14,20] in order to determine the diffusion coefficients and activation energy for Si-Ge interlayer mixing. In one study[20] a number of specimens were analyzed with θ-2θ scans before and after annealing. Samples were heated at several temperatures for varying amounts of time, with 880 °C/9 s and 935 °C/20 s representing the minimum and maximum temperature/time combinations. Concerns have arisen that annealing may effect the state of strain in the SLSs of buffer layers and lead to partial relaxation which will erroneously influence[21,22] the diffusion measurements. The $k_{\alpha 2}$ stripped buffer layer/0-order SL (400) reflections of the $Si_{15}Ge_{15}$

sample before and after annealing are also plotted in Fig. 4. It can be seen that small but noticeable shifts in the buffer layer/SL peaks occur with temperature, and that the shift is present even at the lowest temperature/time combination studied. These shifts represent only a 2–4% change in the total lattice mismatch between the buffer and substrate and are comparable with the degree to which some of the buffer layers were not completely relaxed. As a result, this may reflect additional strain relaxation or dislocation growth (or movement) in either the SL or buffer but the magnitude of the change suggests that it is minor.

B. Cross sectional transmission electron microscopy

Cross sectional TEM images of the nominal 40 ML period SLSs are presented in Fig. 5 and the same general trends that were observed in the XRD data can be seen in these images. A summary of the SL periodicities measured from the XTEM micrographs are presented in Table I. The SL periodicities measured from the XTEM images were comparable with the XRD and Raman values, while the buffer layer thicknesses were consistently lower than the targeted values by 5–25% and were comparable with those derived from the RBS analyses. Based on the number of defects and the parallelism and thickness of the individual layers, the quality of the Si_8Ge_{32} SLS is superior to that of the $Si_{32}Ge_8$ sample, and both are considerably better than the $Si_{20}Ge_{20}$ SLS. Dislocations which affected the lateral parallelism of the layers were present in both the Si_8Ge_{32} and $Si_{32}Ge_8$ structures, but it was noted that those in the Si_8Ge_{32} sample tended to propagate from the buffer layer into the SLS, whereas in the $Si_{32}Ge_8$ sample the upper portion of the buffer was relatively free of dislocations and their growth in the SLS was initiated at the buffer interface. This suggests that the state of strain at the upper surface of the buffer and in the SLS were not well matched in the $Si_{32}Ge_8$ sample since misfit dislocations were initiated in the SLS, but there is no strong XRD evidence to support this interpretation since the SLS and buffer layer appear to be lattice matched well. The quality of the $Si_{20}Ge_{20}$ sample, in contrast, is much poorer with loop-like dislocations present throughout the buffer and SLS, and the layers in the SLS are very wavy in appearance. The upper surface of the buffer layer in this sample is also somewhat irregular and this may have influenced the subsequent growth of the SLS.

Similarly, the XTEM images of the nominal 20 ML SLS (Fig. 6) support the trends that were observed in the XRD data. In this case, however, the $Si_{16}Ge_4$ SLS has the highest quality, followed by the Si_4Ge_{16} and $Si_{10}Ge_{10}$ samples. In general the layers in the 20 ML Si_mGe_n SLSs were parallel and uniform in thickness, although some dislocations were observed. All the Si_mGe_m samples, however, had the poorest quality with the buffer layers having irregular upper surfaces and the SLS layers being wavy in appearance. The differences in quality between the Si-rich and Ge-rich Si_mGe_n SLS are reversed in the 40 ML and 20 ML samples and this may reflect individual growth conditions. The high angle θ-2θ XRD data, however, did suggest that the degree of strain matching between the buffer and SLS in the Si_4Ge_{16} sample was imperfect.

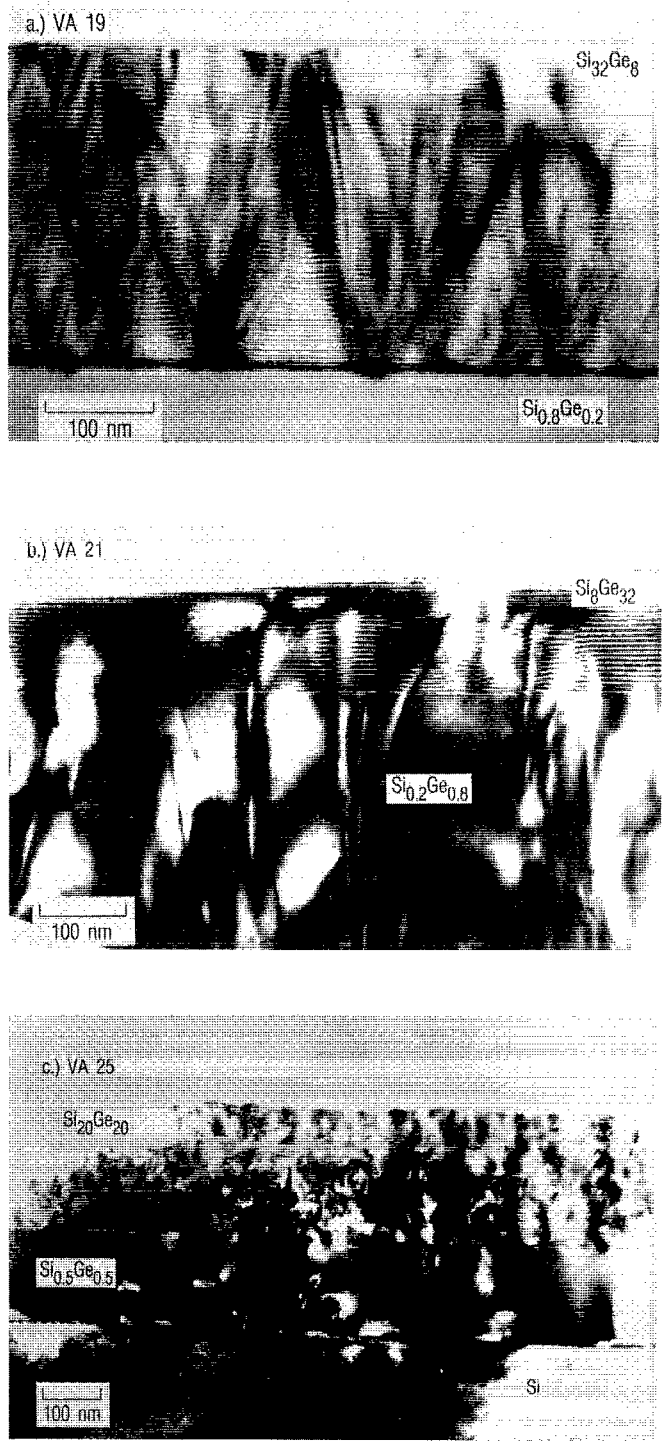

FIG. 5. Bright field cross sectional transmission electron micrographs of nominal 40 monolayer period SLSs.

V. DISCUSSION

A series of Si_mGe_n superlattices has been studied by XRD, XTEM, and Raman spectroscopy and in most instances the as-grown structures matched the targeted val-

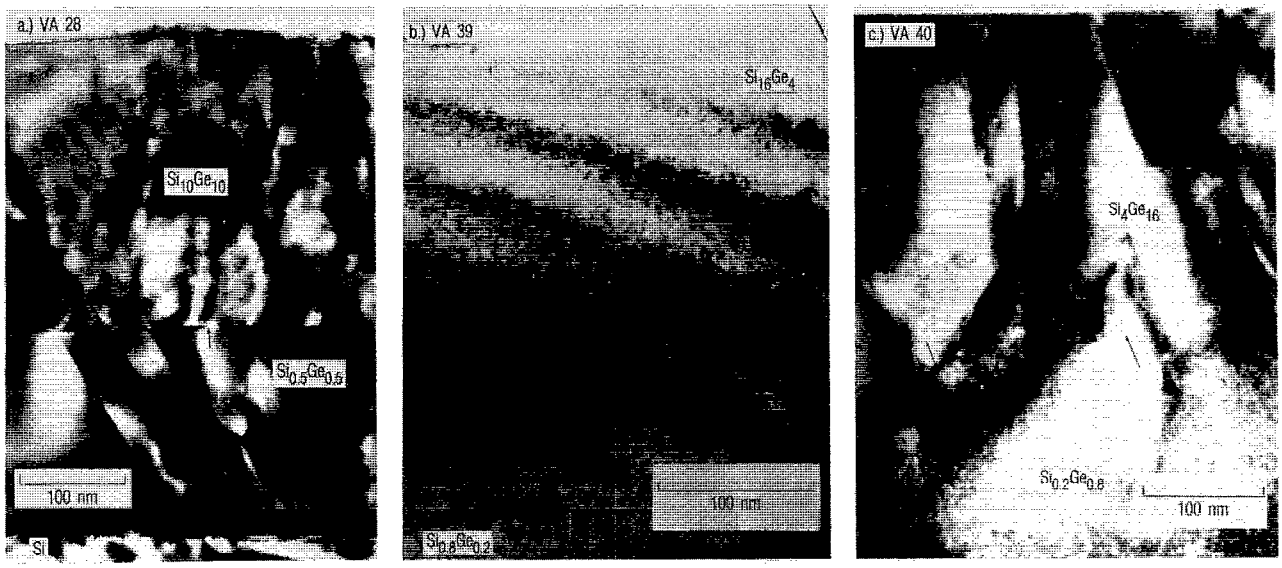

FIG. 6. Bright field cross sectional transmission electron micrographs of nominal 20 monolayer period SLSs.

ues reasonably well (Table I). The measured SLS periodicities agreed with the target values to within 10% in most cases, although deviations of 20% were observed for two Si_mGe_m samples. The measured compositions of the buffer layers in most cases closely matched the targeted values, but those with the lowest Ge contents ($x = 0.20$) deviated the greatest, with compositions 25% lower than expected. A limited number of buffer and SLS compositions derived by RBS agreed reasonably well with the XRD data and confirmed the assumption that the buffer layers were nearly completely (95–97%) to completely relaxed. In the majority of samples the SLSs appeared to be adequately lattice matched to the buffer layer as indicated by the superposition of the (400) buffer layer and 0-order SL reflections. In the two samples with the greatest lattice mismatch (i.e., $Si_{10}Ge_{10}$ and $Si_{15}Ge_{15}$), however, the measured periodicities were significantly different from the targeted values, suggesting that the growth had not been well controlled. The XRD data indicated that the qualities of the SLS structures were greatly dependent on the composition of the buffer layer on which they were grown, even though the structures of the SLSs were tailored for strain symmetrization and lattice matching with the buffer layers in each case. The quality of the Si_mGe_m SLSs were considerably poorer than Si_mGe_n structures as indicated by the number of orders and the FWHMs of the superlattice reflections in the θ-2θ scans and rocking curves. While the quality of Si_mGe_n SLSs were by far the best, significant numbers of defects were nevertheless present, since the superlattice reflections observed in the rocking curves were weak and displayed broad peaks suggestive of dislocation densities on the order of 1×10^9 cm^{-2}. Dislocations are not the only defects that have been observed in the structures and other factors such as nonparallelism of the layers and nonuniform strain symmetrization or relaxation throughout the structure could equally degrade the appearance of the rocking curves. XTEM observations have verified the majority of conclusions derived from the XRD analyses and have shown that the upper surfaces of the buffer layers on which the Si_mGe_m SLS structures were grown were very irregular and that the SLSs contained significant numbers of defects, including misfit and threading dislocations and irregular nonparallel layers. The quality of the Si_mGe_n SLSs was considerably better, with the surfaces of the buffer layers being much smoother, but many of the other defects were still present, although in much lower numbers.

ACKNOWLEDGMENTS

This work was supported in part by the Aerospace Sponsored Research Program. The work at the California Institute of Technology is supported by the National Science Foundation Materials Research Group Program Grant DMR-8811795. The work at the University of California is supported by the Semiconductor Research Corporation and the Army Research Office. The authors wish to thank W. S. Liu and M-A. Nicolet for the RBS analyses.

[1] R. P. G. Karunisiri and K. L. Wang, J. Vac. Sci. Technol. B **9**, 2064 (1991).
[2] E. Kasper, H. Kibbel, H. Jorke, H. Brugger, E. Friess, and G. Abstreiter, Phys. Rev. B **38**, 3599 (1988).
[3] G. Abstreiter, K. Eberl, E. Friess, W. Wegscheider, and R. Zachal, J. Cryst. Growth **95**, 431 (1989).
[4] E. Kasper, H. Kibbel, and H. Presting, Thin Solid Films **183**, 87 (1989).
[5] J. Hornstra and W. J. Bartels, J. Cryst. Growth **44**, 513 (1978).
[6] D. J. Lockwood, J. M. Baribeau, and P. Y. Timbrell, J. Appl. Phys. **65**, 3049 (1989).
[7] M. Halliwell, M. Lyons, S. Davey, M. Hockly, and C. Tuppen, Semicond. Sci. Technol. **4**, 10 (1989).
[8] D. C. Houghton, D. D. Perovic, J. M. Baribeau, and G. C. Weatherly, J. Appl. Phys. **67**, 1850 (1990).
[9] J. M. Vandenberg, J. C. Bean, R. A. Hamm, and R. Hull, Appl. Phys. Lett. **52**, 1152 (1988).
[10] D. B. McWhan, *Synthetic Modulated Structures* (Academic, New York, 1985), Chap. 2, p. 43.

[11] V. S. Speriosu and T. Vreeland, Jr., J. Appl. Phys. **56**, 1591 (1984).
[12] H. P. Klug, and L. E. Alexander, *X-ray Diffraction Procedures*, 2nd ed. (Wiley, New York, 1974) pp. 274–277.
[13] M. Rytov, Sov. Phys. Acoust. **2**, 68 (1956).
[14] S. J. Chang, V. Arbet, K. Wang, R. C. Bowman, Jr., P. M. Adams, D. Nayak, and J. Woo, J. Electron. Mater. **19**, 125 (1990).
[15] S. J. Chang, C. F. Huang, M. A. Kallel, K. L. Wang, R. C. Bowman, Jr., and P. M. Adams, Appl. Phys. Lett. **53**, 1835 (1988).
[16] R. C. Bowman, Jr., P. M. Adams, C. C. Ahn, S. J. Chang, V. Arbet, and K. Wang, Mater. Res. Soc. Symp. Proc. **160**, 101 (1990).
[17] L. V. Azaroff, *Elements of X-ray Crystallography* (McGraw Hill, New York, 1968), p. 244.
[18] V. S. Speriosu, J. Appl. Phys. **52**, 6094 (1981).
[19] J. Ladel, A. Zagofsky, and S. Pearlman, J. Appl. Crystallogr. **8**, 499 (1975).
[20] R. C. Bowman, Jr., P. M. Adams, S. J. Chang, V. Arbet-Engels, and K. L. Wang, Mater. Res. Soc. Symp. Proc. **220**, 161 (1991).
[21] S. M. Prokes and K. L. Wang, Appl. Phys. Lett. **56**, 2628 (1990).
[22] J. M. Baribeau, R. Pascual, and S. Saimoto, Appl. Phys. Lett. **57**, 1502 (1990).